



A biviscous modified Bingham model of snow avalanche motion
by Jimmie Duane Dent

A thesis submitted in partial fulfillment of the requirements for the degree of DOCTOR OF
PHILOSOPHY in Civil Engineering
Montana State University
© Copyright by Jimmie Duane Dent (1982)

Abstract:

Contained in this thesis is a description of snow avalanche dynamics. This information is gained from the researches of others and from an experimental program that is described within. Tests were carried out in which 2.1 m³ volumes of snow were decelerated to a stop from 18 m/s on a flat level snow covered runout. Data concerning leading edge position versus time and flow velocity versus depth were collected.

Based upon this information a biviscous modified Bingham flow model is proposed and developed. This flow model consists of a constitutive relation that is linear between the stress and velocity gradients over two distinct regions. There is a region of high viscosity, for low stresses, where little deformation will take place and a second region with a much lower viscosity that operates for stresses above a specified level.

This model, in the form of a finite difference computer code, is used to simulate the results of the snow flow tests. In carrying out this modeling, values of the parameters that appear in the biviscous flow law are evaluated.

A BIVISCOUS MODIFIED BINGHAM MODEL OF SNOW AVALANCHE MOTION

by

JIMMIE DUANE DENT

A thesis submitted in partial fulfillment
of the requirements for the degree

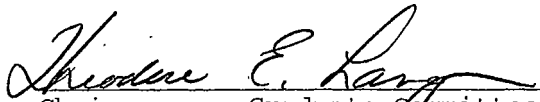
of

DOCTOR OF PHILOSOPHY

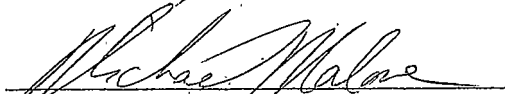
in

Civil Engineering

Approved:


Chairperson, Graduate Committee


Head, Major Department


Graduate Dean

MONTANA STATE UNIVERSITY
Bozeman, Montana

June, 1982

ACKNOWLEDGMENT

This work was made possible through grants from the U. S. Department of Agriculture, Forest Service (cooperative agreement Nos. Rm-16-778-CA, Rm-16-884-CA, Rm-81-165-CA) and from the Montana State University Computing Center. The support from these agencies, and in particular Mr. Mario Martinelli, Jr. of the Forest Service and Range Experiment Station and Mr. Robert Motsch and Mr. Phillip Adolf of the M.S.U. Scientific Subsystems computing facility is gratefully appreciated. Also this work would not have been possible without the facilities of the Civil Engineering and Engineering Mechanics Department and Mr. Theodore Williams.

The author would especially like to thank Dr. Theodore Lang for his help and guidance in the preparation of this thesis, for the many hours spent in the field shoveling snow and for the many hours spent listening and counseling.

To all those people who are not mentioned here, but who have participated in some way in this research, I would also like to say thank you.

TABLE OF CONTENTS

	<u>Page</u>
VITA.	ii
ACKNOWLEDGMENTS	iii
LIST OF FIGURES	vi
ABSTRACT.	ix
 CHAPTER	
I. INTRODUCTION	1
II. A DESCRIPTION OF AVALANCHE MOTION.	3
Observations	3
Measurements	4
III. HISTORICAL ANALYSIS OF AVALANCHE MOTION.	11
Open Channel Flow.	12
Center of Mass Motion.	17
Linear Viscous Model	19
Bingham Model.	20
Granular Theories.	24
IV. FIELD TEST PROGRAM	26
The Test Facility.	26
Observations and Measurements.	29
Window Tests	42
Discussion of Test Results	42
V. BIVISCOUS BINGHAM MODEL	47
Linear Viscous Model	47
SMAC	49
Linear Viscous Model Results	56
Bingham Model.	58
Biviscous Bingham Model.	60
BVSMAC	68
Biviscous Modeling Results.	84

Table of Contents (Continued)	<u>Page</u>
VI. SUMMARY AND CONCLUSIONS.	96
LIST OF REFERENCES.	101
APPENDICES.	106
A. BVSMAC Fortran Computer Code.	106
B. Time Sequence Particle Plots of BVSMAC Calculation of Flowing Snow Test.	132
1. $\tau_{o/\rho} = 2.2 \text{ m}^2/\text{s}^2$, $\nu = .002 \text{ m}^2/\text{s}$, $\nu' = 0.10 \text{ m}^2/\text{s}$	133
2. $\tau_{o/\rho} = 3.0 \text{ m}^2/\text{s}^2$, $\nu = .010 \text{ m}^2/\text{s}$, $\nu' = 0.20 \text{ m}^2/\text{s}$	144
3. $\tau_{o/\rho} = 1.0 \text{ m}^2/\text{s}^2$, $\nu = .010 \text{ m}^2/\text{s}$, $\nu' = 0.10 \text{ m}^2/\text{s}$	154
C. Viscous Deformation of a Rectangular Block	164
1. $\nu = .001 \text{ m}^2/\text{s}$	165
2. $\nu = .010 \text{ m}^2/\text{s}$	168
3. $\nu = .100 \text{ m}^2/\text{s}$	172
4. $\nu = .200 \text{ m}^2/\text{s}$	177

LIST OF FIGURES

	<u>Page</u>
1. Profile of an avalanche derived from pressure sensors (Schearer 1980)	9
2. Shear stress of granular snow on an over-riding surface-roughened steel plate versus speed of the plate. (Lang et al. 1981)	23
3. Schematic of field test facility.	27
4. Photograph of field test facility	28
5. Glass window used to measure velocity profile	30
6. Dump geometry, test No. 3-2-23-80	31
7. Power Cloud	33
8. Dump geometry, test No. 2-2-23-80	35
9. Leading edge position versus time, test No. 2-2-23-80	36
10. Debris distribution, test No. 2-2-23-80	37
11. Debris distribution, test No. 3-2-23-80	38
12. Dump geometry, test No. 1-2-25-80 (Block Test).	40
13. Debris distribution, test No. 1-2-25-80	41
14. Cross section of debris, chunk test 1-2-25-80	43
15. Cross section of debris, chunk test 1-2-25-80	44
16. Data points of particle speed versus depth of flow.	45
17. SMAC computing grid	52
18. SMAC method of specifying the tangential boundary condition at a rigid wall.	54
19. One dimensional form of the Bingham and Biviscous constitutive laws.	63

List of Figures (Continued)	<u>Page</u>
20. Mohr's circles for the rotational transformation of the deviatoric stresses and the velocity gradients.	67
21. Flow between parallel plates; geometry stress and velocity gradient.	71
22. BVSMAC particle plot sequence for the solution to the flow of a Bingham material between parallel plates: $\tau_0/\rho = 0.30$, $v = 0.20$, $v' = 2.0$	74
23. Steady state velocity profile, comparison between analytical and numerical solutions	78
24. BVSMAC particle plot, flow between parallel plates at $t = 1.0$ s; $\tau_0/\rho = 0.30$, $v = 0.20$, $v' = 4.0$	79
25. BVSMAC particle plot, flow between parallel plates at $t = 1.0$ s; $\tau_0/\rho = 0.60$, $v = .20$, $v' = 2.0$	80
26. Constitutive relations for the Biviscous model simulations of the flow between parallel plates	81
27. BVSMAC particle plot, flow between parallel plates $t = 1.0$ s; $\tau_0/\rho = 0.60$, $v = 0.10$, $v' = 2.0$	83
28. Input flow configuration for BVSMAC simulation of snow test 2-2-23-80.	86
29. Constitutive relations that adequately modeled the leading edge motion of snow test 2-2-23-80	88
30. Leading edge position versus time; comparison between experiment and BVSMAC ($\tau_0/\rho = 2.2 \text{ m}^2/\text{s}^2$, $v = .002 \text{ m}^2/\text{s}$, $v' = 0.10 \text{ m}^1/\text{s}$)	90
31. Velocity profile comparison between snow test and BVSMAC calculations for various combinations of BVSMAC parameters	91

List of Figures (Continued)

Page

32. Final debris depth profile; comparison between experiment and BYSMAC model.	93
--	----

ABSTRACT

Contained in this thesis is a description of snow avalanche dynamics. This information is gained from the researches of others and from an experimental program that is described within. Tests were carried out in which 2.1 m³ volumes of snow were decelerated to a stop from 18 m/s on a flat level snow covered runnout. Data concerning leading edge position versus time and flow velocity versus depth were collected.

Based upon this information a biviscous modified Bingham flow model is proposed and developed. This flow model consists of a constitutive relation that is linear between the stress and velocity gradients over two distinct regions. There is a region of high viscosity, for low stresses, where little deformation will take place and a second region with a much lower viscosity that operates for stresses above a specified level.

This model, in the form of a finite difference computer code, is used to simulate the results of the snow flow tests. In carrying out this modeling, values of the parameters that appear in the biviscous flow law are evaluated.

CHAPTER I

INTRODUCTION

Snow avalanches represent a significant hazard in the mountainous regions of the world. Every year many people are killed and millions of dollars of damage are done by avalanches. The United States alone, averages seven deaths and \$300,000 in property destruction annually. (Perla and Martinelli, 1975). The European Alpine countries, because of their much more densely settled mountain regions have a much more severe problem. Single avalanches have taken as many as 96 lives in the United States and an avalanche consisting of ice, snow, and earth completely buried a village in the Peruvian Andes in 1970, killing over 20,000 people.

As activity increases in the mountainous regions of the world, the potential for avalanche destruction mounts. It thus becomes increasingly important to be able to identify avalanche hazards. Avalanche paths and their runout zones must be mapped in those regions people frequent, so that construction in hazardous areas can be minimized. In those instances where building in an avalanche path cannot be avoided, for example, roads and bridges, engineering design criteria must be established to minimize potential danger. This can take the form of construction of defensive structures for protection, or designing the primary structure itself to withstand anticipated avalanche forces. In either case, it is necessary to be able to predict avalanche motion and the forces that the avalanche would exert on the

structure under consideration. It is these concerns that motivate the study of avalanche dynamics. Through an understanding of the mechanics of flowing snow, predictive models may be developed that will allow engineers to build safely in avalanche hazard areas.

Contained in this thesis is a description of avalanche mechanics. Much of this information is observational in nature, since great difficulty is encountered in attempting to instrument and measure full scale avalanche motion. From this understanding of avalanches, a flow model is proposed and developed. This model, based upon the classical equations of continuum mechanics, may be used to predict avalanche motion and impact forces. Analytical data on moving snow are scarce; therefore, to test the model, it was necessary to institute a field program for the collection of data. The field data were used to help verify and then to calibrate the flow model. This provided a source of analytic, as well as qualitative information on flowing snow that has led to a better understanding of the mechanics of snow flow. The model may now be used to predict avalanche motion and impact forces.

CHAPTER II

A DESCRIPTION OF AVALANCHE MOTION

Observations

A snow avalanche can range from a few snow particles rolling and bouncing down a slope to a massive assemblage of ice, snow, and earth, moving with enough velocity to destroy virtually anything in its path. The majority of avalanches are of the former type; harmless sluffs of small volumes of snow that occur as new snow is deposited on mountain slopes. Large avalanches occur much less often and only achieve destructive potential when the volume of snow reaches about 1000 m^3 . These destructive avalanches typically start high on a mountain side in snow catchment areas called starting zones. As snow is deposited on these 30 to 45 degree slopes, the snow load eventually exceeds the strength of the bonds holding the snow in place. Volumes of snow upwards of 10^5 m^3 can then be released at one single time. The released snow may be made up of new cohesionless snow that has recently been deposited, in which case the resulting avalanche is a loose snow avalanche. If the snow has resided on the ground for a period of time, it will have sintered into a solid matrix. When it then starts to move, this slab avalanche initially moves as a large rigid block that immediately begins to break into pieces. Finally, if the snow pack has warmed and there is free water in the snow when it is released, a wet snow or slush avalanche results. Combinations and variations of these

avalanches, of course, also may be observed.

Once initiated the avalanche gains speed as it flows down the avalanche track. The blocks that may have been present at release begin to break up. They tumble and collide with each other rounding corners, and reducing their sizes. The smaller snow particles can be thrown into the air by collisions with other particles, creating a dust cloud that may completely surround the flow. It is even possible for loose snow avalanches to become entirely airborne, with all the snow being air entrained so that there is no central flowing core. However, the majority of avalanches consist of a dense flowing core that contains most of the momentum and is responsible for the high damage potential. This core is surrounded by a large diffuse dust cloud that makes observation of the flowing core difficult. As a large avalanche continues to move down the mountain its velocity may reach upwards of 50 m/s. Typical flow speeds however, are more in the range of 20-40 m/s. The avalanche keeps flowing until the slope angle decreases to a point where gravity can no longer sustain the motion or until some obstacle is encountered.

Measurements

The description of avalanche motion involves specifying such parameters as velocity, density, and volume, as fundamental variables. These quantities must be known as functions of space and time to totally define the flowing system. But, because of the formidable nature of

snow avalanches and their hostile environment, even the simplest measurements have proven very difficult to perform. As a result, much of the information about avalanches has been gathered by examining the debris after it has stopped. Mass estimates, type of snow, and particle sizes can all be ascertained. The slope profile can be measured and simple energy analysis used to determine average friction values and average flow velocities (Körner 1981). Data collection on moving avalanches was at first limited to eye witness accounts and their estimates of speed and length of time that the avalanche ran. A few avalanches were timed to yield average velocity values. Only in recent years have attempts been made to collect time dependent data. These efforts have mostly centered on the measurement of avalanche velocities, of which most measurements have been only of the leading edge of the avalanche. For example, Shoda (1966), LaChapelle and Lang (1979), and Martinelli et al. (1980) have all used motion picture photography to gather this information. They filmed avalanches as they descended a slope and then analyzed the film to determine the number of frames necessary for the front of the avalanche to traverse known distances between landmarks. This is a tedious procedure that is fraught with many difficulties. Among them are parallax errors, badly spaced or poorly defined landmarks, and obscurement of the flowing mass by the powder dust cloud. Photogrammetric techniques eliminate the parallax and landmark difficulties at the expense of more effort for

data collection and reduction. Bruikhanov (1967) in the Soviet Union and Brugnot (1980) in France have successfully employed this method to measure the time-dependent leading edge velocity for several full scale avalanches. There is only in existence then a very limited number of data sets providing avalanche leading edge velocities.

Measurements of flow velocities in avalanches at points other than the leading edge are extremely rare. Some measurements have been made by Schearer (1973), Schearer and Salway (1980) and Shimizu et al. (1973, 1975, 1977, 1981). These researchers mounted sets of pressure transducers in avalanche paths. By correlating the pressure signals observed in separate sensors and the time difference between the signals, internal velocities could be calculated. Only sporadic measurements could be made, however, due to the difficulty in finding correlations between sensor signals.

A potentially powerful technique for measuring velocities lies in the use of microwave radar. Gubler (1980) has used this technique to measure leading edge velocities and is currently experimenting with the use of active and passive sensors imbedded in the avalanche flow. It is hoped that development of this system will lead to the capability of measuring internal flow velocities.

Because velocity data is so hard to gather by field measurements, physical modeling has provided another means of obtaining useful avalanche data. Powder avalanches in particular have lent themselves to

this type of analysis. In scale modeling, dynamic similarity must be maintained and boundary conditions faithfully reproduced. Dynamic similarity is achieved by matching certain characteristic dimensionless numbers that involve the flow parameters. In the case of powder avalanche modeling it is the densimetric Froude number, which is the ratio of inertial forces to gravitational forces, that must be matched. In addition, the Reynolds number, which is the ratio of inertial to viscous forces must be maintained high so that viscous effects are negligible. Hopfinger and Tochan-Danguy (1975) and Tochan-Danguy and Hopfinger (1977) were able to match the Froude number of powder avalanches by using the gravity flow of salt solutions. They constructed a three meter long inclined tank to allow a salt brine to flow under a less dense ambient fluid. The qualitative results of this model strongly resemble the motion of the natural event. Quantitative data, however, was limited.

As sparse as data is for velocities, it is much better than the data available for snow density within the flowing avalanche. Direct density measurements have been very difficult to make. Eyber-Berard et al. (1980) attempted to use gamma rays to obtain some average density measurements in flowing snow, but they obtained little useful data. Indirect evidence based on flow depths, has also been used to estimate the average snow density in an avalanche. These estimates range from $60-90 \text{ kg/m}^3$ for dry snow avalanches to $300-400 \text{ kg/m}^3$ for wet snow

avalanches, Schaerer (1975). Schaerer and Salway (1980) concluded from evidence gathered from their pressure gauges located at Rogers Pass in British Columbia "that well-developed dry snow avalanches...consist of three stratified components: dense flowing snow at the bottom, light flowing snow, and powder snow" at the top (Fig. 1). They go on to say that the dense zone was 0.5 to 1.2 m deep and formed the principle mass of the avalanche. The light flowing snow, with an average density from 10 to 30% of that of the dense zone, consisted of a mixture of powder and lumps of snow of up to 60 mm in diameter. Their speculation is that this 1 to 5 m layer of light snow is the result of lumps being tossed upwards from the surface of the dense flowing snow by the turbulent motion at that surface. In the runout zone the light flow is often observed to separate from the dense flow either at bends in the avalanche track or during rapid deceleration. The third component of the avalanche reported by Schaerer and Salway is the powder cloud which could not be detected by their instruments, but was observed visually. Systematic direct measurements of snow density in avalanches will probably have to await further development of remote sensing techniques.

There is, in general, a lack of documentation of avalanche flow. Very little time-dependent data is available and virtually no systematic measurements have been made. Also lacking is experimental data under controlled flow conditions, detailed data that could be used for evaluation of theoretical models. Therefore, it was necessary to initiate

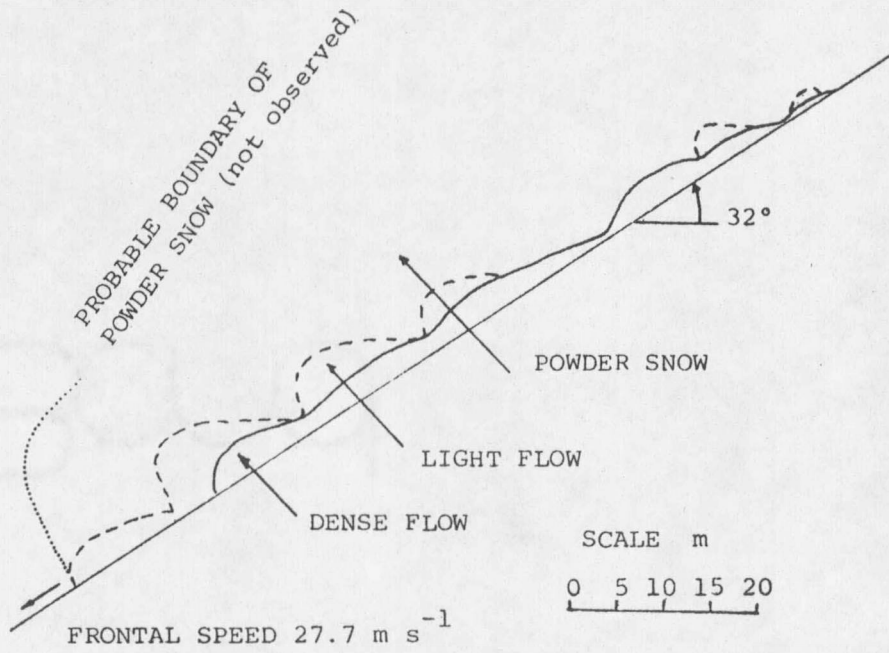


Figure 1. PROFILE OF AN AVALANCHE DERIVED FROM PRESSURE SENSORS (SCHAERER 1981).

a field test program for the express purpose of documenting snow flowing under controlled conditions. This effort is described in Chapter IV. The next chapter gives an historical review of the development of snow avalanche theory.

CHAPTER III

HISTORICAL ANALYSIS OF AVALANCHE MOTION

If one were to try to characterize snow avalanches in general terms, a description might read: 'A snow avalanche is the transient, 3-dimensional motion of a variable mass system made up of a non-rigid, non-rotund, non-uniform assemblage of cohesive granular snow fragments flowing down a non-uniform slope of varying surface resistance.' The driving force in an avalanche is the force of gravity, but the resistive forces are dependent upon the interactions between the individual snow fragments. Even if the form of the interaction forces were known, the large number and highly variable nature of the particles would make analysis unmanageable, except in some statistical sense. Given, then, that the exact mechanical solution to the avalanche motion problem may be impossible, it is also unnecessary. The motion of individual snow fragments is only of limited interest. For most purposes the time and spacial transients are small. A possible exception would be the impact of an individual snow clod upon an area of similar or smaller size. In general, it is the overall motion - the average motion, in some sense - of the avalanche that is of interest. Approximations to the mechanics of the fragment interactions must be made so that analysis can be carried out. In this way, some appropriate average velocity may be determined from which runout distances and impact forces can be calculated. It is generally true that the more realistically the interaction forces are modeled, the more accurate and general will be the analytical

solution. It has been the objective of the avalanche dynamicist to formulate avalanche flow models simple enough to solve, yet complicated enough to include as much of the mechanical behavior of the avalanche as possible.

Open Channel Flow

Among the first to present an analytical formulation for avalanche flow was A. Voellmy in his classic monograph presented in 1955. Voellmy based his analysis on the equations developed to describe open-channel fluid flow. He extended the open-channel hydraulics approach, with all its implicit assumptions, to the flow of snow on a mountain slope. Voellmy, and many others since him, have based their theories on the observation that snow avalanches seem to "flow". That is, as the material deforms, it conforms to the slope, and is often seen to flow around obstacles. This motion is much like the movement of water along a streambed - hence the analogy with open channel hydraulics. Implicit in the assumptions of this approach is that flowing snow behaves as a fluid. In most continuum mechanical theories, fluids are considered to be continuous, homogeneous, and isotropic. That is, any granular nature of the material is ignored, and spatial variations in the fluid are neglected. Furthermore, hydraulics deals with materials that can be considered incompressible. The degree to which these considerations influence snow avalanche movement determines the extent to which an incompressible fluid model can give useful results. The

incompressible fluid model does, however, provide for simple analysis. Using a continuum mechanical theory, the avalanche flow problem is reduced to finding point values for the stresses within the material. This can be done most easily by using a momentum-balance approach. The stresses must then be related to the deformation by a constitutive equation that takes into account the properties of the fluid.

The open channel hydraulics analysis that Voellmy applied, contains, in addition to the fluid assumptions, approximations related to fluid motion in an open channel. Chief among these approximations is that the flow is steady: that is, that there is no time-dependence to the motion. It is assumed that the avalanche quickly accelerates on a constant slope to a terminal velocity and thereafter exhibits steady motion. The momentum-balance equation is then commonly integrated over the slope-normal cross sectional area so that only the boundary stresses need be considered. The dependent variable becomes the average velocity of the material in cross-section. In addition, a uniform motion is usually assumed, so that the flow variations along the slope can be neglected. Under these assumptions, the momentum balance equation becomes the equilibrium condition,

$$\tau = \rho g h \sin\theta \quad (3.1)$$

in which τ is the resistive shear stress at the fluid boundary, ρ is the average fluid density, g is the acceleration of gravity, h is the

flow depth, and θ is the slope angle. In order to derive an expression for the velocity of the flow, an equation relating the velocity to the stresses on the boundary must be introduced. For this constitutive equation Voellmy used the Prantl mixing length approximation (Pao 1961), which for turbulent fluid flow, in which the velocity and stresses at any point fluctuate randomly, yields the following boundary drag:

$$\tau = k_1 v^2 \quad (3.2)$$

However, Voellmy also noted that a minimum slope angle was required for an avalanche to start, so he proposed to modify this equation by adding a constant.

$$\tau = k_1 v^2 + \mu g h \rho \cos \theta \quad (3.3)$$

The form of the additional term in this equation is the same as that of a conventional coulomb friction force in which μ is the coefficient of friction. The addition of the friction term was found to be necessary, because of the cohesion or locking property that snow exhibits; a minimum stress-level must be exceeded before deformation occurs. Using equation 3.3 for the shear stress at the avalanche snow surface interface, the momentum balance equation may be solved for the flow velocity yielding

$$v = \sqrt{\xi h (\sin \theta - \mu \cos \theta)} \quad (3.4)$$

where the drag coefficients and the density have been combined into a single parameter ξ . The flow velocity calculated by this equation is the average steady state or terminal velocity that an avalanche is

supposed to attain under uniform conditions on a constant slope. (In the case of channellized flow, the height of the avalanche, h , is often replaced by the hydraulic radius, R , which is defined as the ratio of the cross-sectional area to the wetted perimeter.)

To calculate runout distances, the avalanche path must be divided into three parts: the starting zone, where the avalanche is initiated and accelerates; the avalanche track, with a constant slope which allows steady-state flow equations to be applied; and the runout zone, where the slope of the track has decreased to allow the avalanche to decelerate to a stop. If it is assumed that the avalanche enters a constant-slope runout zone with the velocity calculated from the steady-state conditions of the track flow, the runout distance S , can be found from a simple energy-balance equation. The equation Voellmy derived is

$$S = v^2 / [2g(\mu \cos \theta - \tan \theta) + v^2 g / \xi h_m] \quad (3.5)$$

in which h_m is the mean deposition depth. By applying these equations to avalanche paths, avalanche runout may be calculated. The usual procedure is to subjectively break the avalanche track into its three sections. the important point being the transition point into the runout zone. The steady velocity is calculated, from the average slope of the track and then the runout distance is computed from the transition point. The result of the analysis is highly dependent upon exactly how the path is divided and where the transition point is chosen.

Through experience, individuals have become very proficient at choosing these points, and this method has yielded good results. As the avalanche paths become complicated, the application of Voellmy's equations become more difficult. Also, the method is found to be difficult for an inexperienced person to successfully apply.

The material parameters appearing in Voellmy's equations are ξ , the turbulent friction coefficient, and μ , the dry friction coefficient. The value of the coefficient ξ is dependent upon snow type and motion; generally the heavier the snow and the slower the motion the smaller the turbulent coefficient. As speed increases and the snow becomes more powdery ξ becomes larger. The coefficient ξ was said to be in the range 400-600 m/s^2 by Voellmy. Later investigators, Mears (1976), Schaerer (1975), Leaf and Martinelli (1977), Buser and Fruitiger (1980), and Martinelli et al. (1980), have allowed ξ to become as large as 1600 m/s^2 for powder avalanches, and have recommended average values of about 1400 m/s^2 .

Bucher and Roch (1946) were among the first to publish data for the dry friction coefficient, μ . They found that for hard, wet snow sliding slowly over a hard, wet snow surface, the friction coefficient ranged from .1 to .4. Inaho (1941) slid blocks of dry snow over a granular surface and found μ to range from .4 to .6. Heimgartner (1977) measured values for μ from .22 to .39 on a small test slide at Weissfuhjoch, and Sommerhalder (1972) computed a maximum friction coefficient of 0.5 and

an average value of 0.32 from data on snow flowing over snowsheds. Using data reduced from 16 mm movie film, Martinelli et al (1980) computed the friction coefficient for a wet slab avalanche in the runout zone to be from .30 to .35.

Center of Mass Motion

Salm (1966) expanded upon Voellmy's theoretical treatment and derived a time-dependent equation for the velocity of the mass-center of an avalanche. His resistive force was a Taylor series in velocity, truncated after the third term.

$$R = R_0 + R_1 \frac{v}{1!} + R_2 \frac{v^2}{2!} \quad (3.6)$$

The constant term (R_0) represents a dry friction force, R_1 can be attributed to linear viscosity, and the third term is due to turbulent friction and the ploughing of the avalanche into the stationary snow. Salm neglected the second term with respect to the third for high speed flowing avalanches, assuming that the energy dissipated by internal friction (R_1 term) is small compared to the turbulent energy dissipation (the R_2 term). The resulting expression for maximum velocity on a constant slope then took the same form as Voellmy's equation. Salm, also used energy considerations to derive an equation for runout distance. It is a more comprehensive treatment than Voellmy's and includes the possibility of artificial obstacles. The equation is considerably more complicated but it does not contain the troublesome singularity that appears in Voellmy's equation.

Mellor in 1968 presented an analysis similar to that of Salm (1966) except that he considered the possibility of having a variable mass system. The mass was allowed to vary linearly with the avalanche velocity.

$$m = m_0 (1 + kv) \quad (3.7)$$

Here m_0 is the initial avalanche mass and k is an entrainment coefficient. This is an empirical relation based upon a correlation between avalanche mass and velocity. The dynamic equations that result from this analysis are cumbersome and "afford little insight into the effects of entrainment as they stand." (Mellor, 1968).

Perla et al. (1980) also developed a center-of-mass system of equations similar to these models. They included a mass-entrainment term proportional to the square of the speed in the dissipative forces. This term combined with other v^2 terms into a single term with the coefficient D , resulted in an equation of motion that was solved successively over small intervals along the slope. In each interval the slope and friction coefficients were considered to be constant. The expression for the maximum velocity over any interval has the same form as Voellmy's equation for terminal velocity,

$$v_{\max} = \sqrt{\frac{mg}{D} (\sin\theta - \mu\cos\theta)} \quad (3.8)$$

in which m/D replaces Voellmy's ξh . In addition, at the juncture of the two segments, a correction for momentum loss due to the slope transition is included.

Values for the parameters μ and m/D for this model are found in the same way that μ and ξ are found for Voellmy's model. The papers by Perla et al. (1980) and Bakkehøi et al. (1980) discuss and give examples for these parameters.

In another work, Perla (1980) analyzed the effects of snow entrainment that occur at a constant rate per unit length of avalanche travel. "Initially entrainment and drag cooperate to oppose acceleration, but if entrainment continues the mass increase will eventually work against the drag and velocity will increase. However,the velocity boost is only significant given continual entrainment on very long paths."

Linear Viscous Model

A major drawback to the mass-center approach to avalanche dynamics is the lumping of the avalanche mass at a single point. An avalanche is an extended mass of variable density and changing velocity. The use of the center-of-mass equations does not provide any insight into the spatial properties of the flow. The flow depth, for example, may appear as a parameter, but it is never calculated. To account for spatial characteristics, a general stress-deformation relation must be applied over the entire flowing mass. One of the simplest relations is the continuum mechanical representation of a linear viscous fluid, where the flow in two dimensions, is governed by the equation;

$$\tau = \mu \left(\frac{\partial u}{\partial y} + \frac{\partial v}{\partial x} \right) \quad (3.9)$$

Here u and v are the slope parallel and slope normal velocity components, and x and y are the slope parallel and slope normal coordinates.

The constant of proportionality μ , between the shear stress, τ , and the velocity gradient term is called the dynamic coefficient of viscosity.

In addition the kinematic coefficient of viscosity is defined as the dynamic viscosity divided by the mass density, ρ , of the fluid.

When this constitutive relation is substituted into the equation of motion, which is derived from momentum balance considerations, a non-linear partial differential equation results - the Navier-Stokes Equation. For the flow geometries encountered in avalanche motion only computer solutions to this equation can be found, and then only in two dimensions and for incompressible flow. The method of solution and the use of this model is detailed in Chapter 5.

The principle parameter for linear viscous fluid flow, the Newtonian viscosity, has never been measured directly for moving snow. Estimates of this parameter range from the kinematic viscosity of air, $1.5 \times 10^{-5} \frac{\text{m}^2}{\text{s}}$, (Perla, 1980), to the viscosity associated with creep motion $63.4 \frac{\text{m}^2}{\text{s}}$, (Shen and Roper, 1970).

Bingham Model

The linear viscous flow model provides a method for calculating the spatial characteristics of flowing snow. However, it is questionable whether flowing snow obeys a linear constitutive equation. The exact dependence of the internal resistive forces on velocity gradient is not

known. Many have speculated that at low speeds the forces may be linearly viscous and that at higher speeds the forces take on a velocity squared dependence due to turbulent motion (Voellmy 1955, Perla, 1980). Thus at least for flows at low velocity a linear viscous model would seem to be appropriate. However, snow exhibits the granular property of requiring a minimum stress to initiate deformation. Regions of material below that minimum stress level do not deform, they translate as rigid bodies. This is seen clearly in the initiation phases of an avalanche where large chunks of material move as blocks until the internal stresses become large enough to break them apart. The linear viscous equations cannot model this behavior since deformation occurs until all internal stresses are relieved. A block of linear viscous material initially at rest on a horizontal surface will deform until it has completely collapsed to zero height and infinite surface extent.

The simplest mathematical model that exhibits the locking property observed in snow and other granular materials is the Bingham model. In the Bingham model no deformation occurs until the shear stress in the material exceeds a specified value (τ_0), then deformation proceeds as a linear viscous material at a rate proportional to the amount that the stress exceeds τ_0 . The constitutive equation for a Bingham fluid then consists of two parts.

$$\text{For } \tau < \tau_0 \quad \frac{\partial u}{\partial y} + \frac{\partial v}{\partial x} = 0 \quad (3.10)$$

and

$$\text{For } \tau > \tau_0, \mu \left(\frac{\partial u}{\partial y} - \frac{\partial v}{\partial x} \right) = \tau - \tau_0 \quad (3.11)$$

Substitution of this constitutive relation into the equations of motion again yields a partial differential equation. The details of the computer method of solution of this equation is also included in Chapter 5.

Direct measurements of the parameters in the Bingham model, the shear stress (τ_0) and viscosity coefficient, (μ), have not been carried out. However, Bucher and Roch (1946), in measuring the frictional resistance of hard wet snow for speeds between 0.2 and 2.4 m/s, found that the linear fit to their data yielded a constant of proportionality of $475 \frac{\text{N-sec}}{\text{m}}$. If it is assumed that there was a 2 mm layer of granulated snow of density 300 kg/m^3 between the sliding surfaces and that the velocity gradient was linear in this region, then the viscosity in this layer would be about $.003 \text{ m}^2/\text{s}$. Similar tests by Lang et al. (1981), using hard sintered snow over the velocity range 0.1 to 0.25 m/s yielded a viscosity coefficient of $.004 \text{ m}^2/\text{sec}$ and a τ_0 value of 540 N/m^2 (Figure 2). These values are for a very narrow range of slow speeds and will most likely differ at higher speeds, but do serve as possible order-of-magnitude estimates.

The viscosity of fluidized snow has been measured in Japan by Maeno and Nishimura (1979), and Maeno et al. (1980). By passing air upward through a snow column they were able to suspend the snow and create a

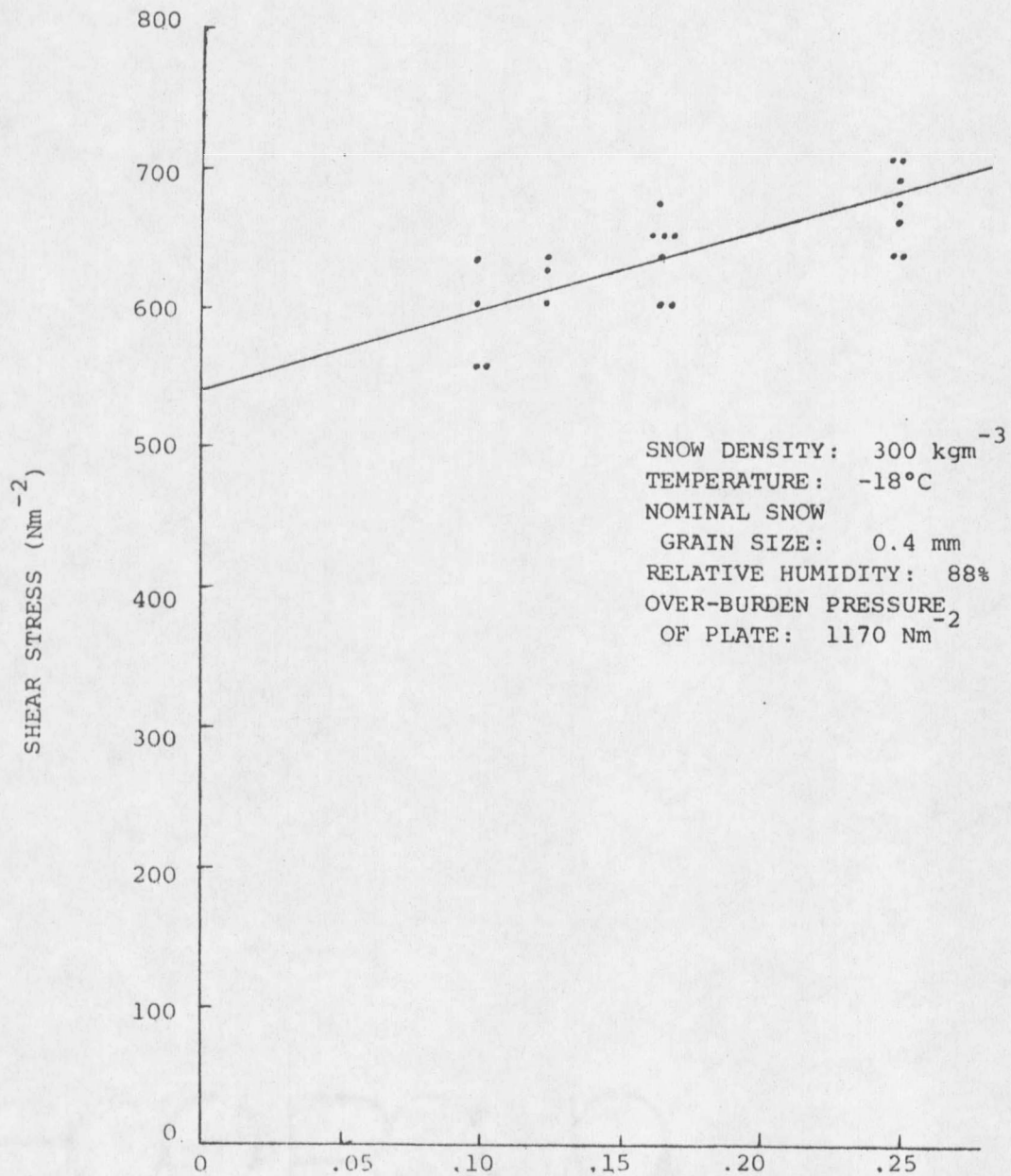


Figure 2. SHEAR STRESS OF GRANULAR SNOW ON AN OVER-RIDING SURFACE-ROUGHENED STEEL PLATE VERSUS SPEED OF THE PLATE. (LANG ET. AL. 1981).

fluidized bed. "The general behavior of the fluidized snow resembled that of a liquid." (Maeno et al. 1980). The dynamic viscosity was measured by standard techniques for a fully fluidized bed and was found to be about $.3 \text{ to } 10^{-3} \text{ N-sec/m}^2$, varying with the particle size and the fluidization velocity. When this number is divided by the density of the snow, values of the kinematic viscosity are found to be in the range $5 \times 10^{-6} \text{ m}^2/\text{s}$ to $.001 \text{ m}^2/\text{s}$. As the fluidization air velocity is decreased below the velocity necessary for complete fluidization, the measured viscosity coefficients rise sharply. At the minimum possible air flow velocity, below which the incomplete fluidized bed becomes unstable and it becomes impossible to measure the viscosity, the measurements yield results in the range $.0001 \text{ m}^2/\text{sec}$ to $.001 \text{ m}^2/\text{sec}$.

Granular Theories

Since flowing snow is made up of granular materials, some of the work in grain flow may eventually be used in snow avalanche models. Mears (1980) has tried to apply some of the results of Bagnold's (1954, 1956) work on cohesionless grain flow to snow. Additional references in the granular material area are articles by Goodman and Cowin (1971, 1972) entitled "A Continuum Theory For Granular Materials" and "Two problems in the Gravity Flow of Granular Materials, a monograph by Savage (1979), "The Gravity Flow of Cohesionless Granular Materials in Chutes and Channels", an article by Nedderman and Laohakul (1980), "The

Thickness of the Shear Zone of Flowing Granular Materials" and a paper entitled "A Micropolar Continuum Theory for the Flow of Granular Materials" by Kanatani (1979). Constitutive equations for granular materials are formulated in these papers and the rheology of grain flow is probed by experimental as well as theoretical techniques. Only a partial list of the work in grain flow has been provided, other investigations either completed or in progress may also have relevance to snow flow. It remains for further research to make use of these theories and formulate better mathematical models for flowing snow. Before much progress can be made in this area however, better data sets must be gathered to check the models against. The next chapter gives the results of one such data collection effort.

CHAPTER IV

FIELD TEST PROGRAM

The Test Facility

A 30° slope near the Bridger Bowl Ski Area in Southwestern Montana was chosen as the location of an experimental test facility. This facility was used to run a number of controlled flow tests of avalanching snow. In these experiments, volumes of prepared snow up to 2.7 m³ were released. This snow descended a 30° slope in a polyethylene lined, one meter radius, semi-circular cross-section track. The polyethylene was utilized to minimize friction to achieve maximum snow velocities. The snow mass accelerated down the length of the track and exited onto a flat-level runout area of packed snow. Using track lengths of 60 m, generated flow speeds of up to 20 m/s at the entrance to the runout area. Upon entering the level runout zone the snow mass decelerated and came to rest. The runout was marked off in one meter increments and a 16 mm movie camera was used to record this phase of the motion. It was the deceleration phase of the snow motion that constituted the snow flow test. A schematic and photograph of the test facility is shown in Figures 3 and 4.

The snow used in the tests ranged in density from 250 to 300 kg/m³. The ambient temperatures on days of testing were always below 0°C, with the skies overcast. The snow was released from a polyethylene lined plywood box by unlocking a hinged door. The mass of snow then

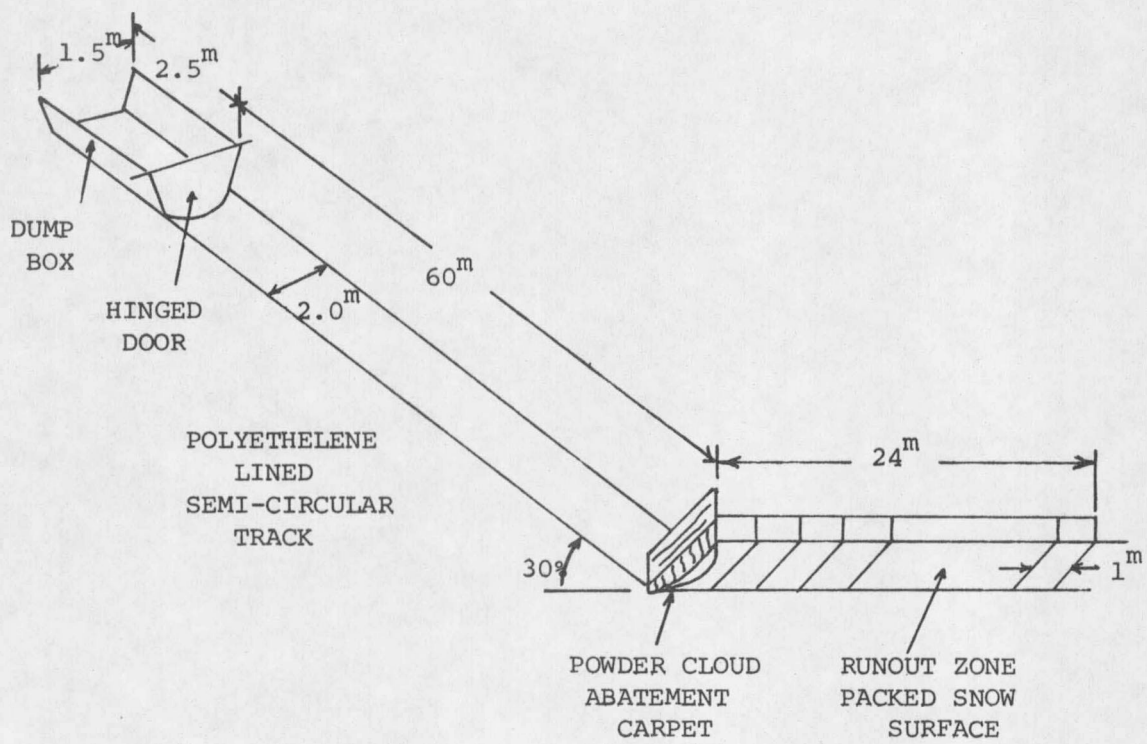


Figure 3: SCHEMATIC OF FIELD TEST FACILITY.



Figure 4: PHOTOGRAPH OF FIELD TEST FACILITY.

accelerated as a semi-rigid body. At the entrance to the runout zone a piece of carpeting was installed just above the track in an attempt to reduce the dust cloud that always accompanied the flowing snow. Depth gauges at the entrance to the runout zone and along the track were used to monitor the depth of flow. In addition, the final debris pile was cross-sectioned and the depth profile was measured.

An attempt also was made to measure the velocity profile as a function of depth at one point in the decelerating flow. This was accomplished by placing a glass window in the runout zone and filming the flow as it passed in front of the window. Marker particles and dye were injected into the snow just prior to reaching the window to enhance visibility. A photograph of this facility is shown in Figure 5.

Observations and Measurements

A number of tests were run on this experimental setup during the winter of 1979-80. For each of these tests the dump box was filled with sifted snow, snow chunks, or combinations of both. In addition, powdered dye was added to the snow at specific locations in the release dump. One such release setup is shown in Figure 6. Upon release, the snow mass accelerated down the polyethelene track and was observed to spread slowly longitudinally. This spreading appeared as crevices formed in the snow. Deformation was also observed, caused mostly by irregularities in the track. As the mass spread, its depth diminished correspondingly.

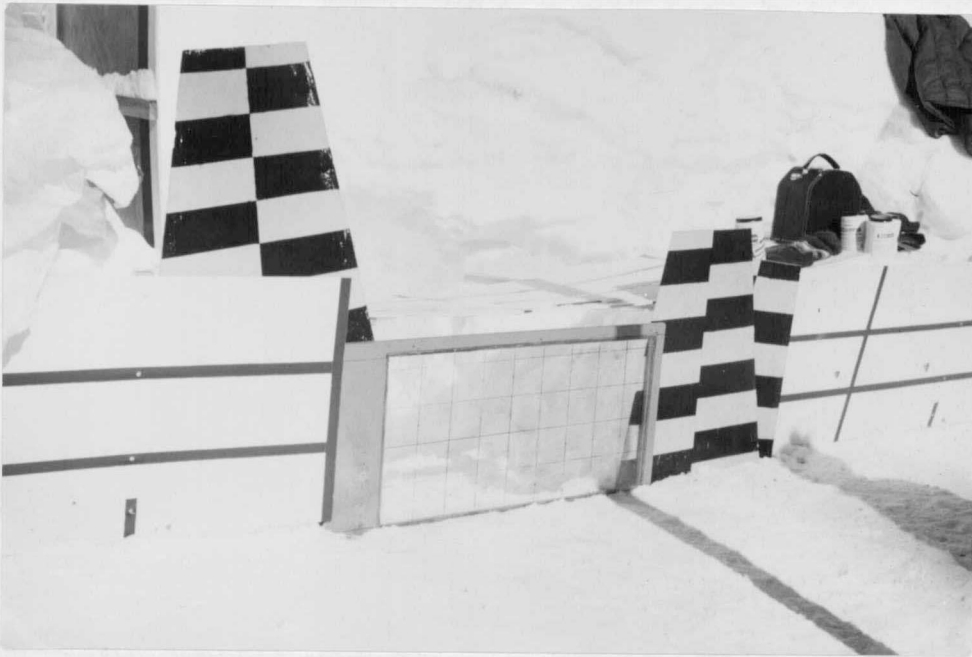


Figure 5: GLASS WINDOW USED TO MEASURE VELOCITY PROFILE.

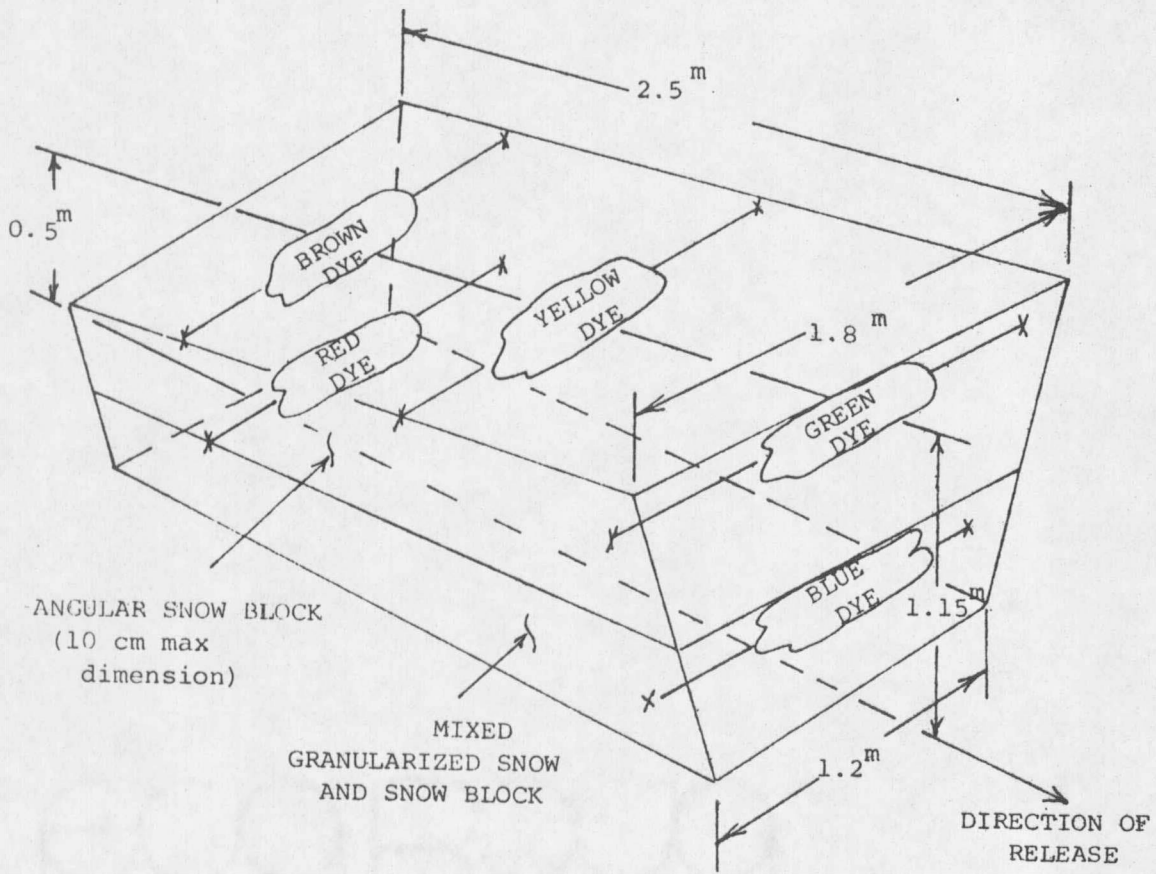


Figure 6: DUMP GEOMETRY, TEST NO. 3-2-23-80.

The flow eventually reached speeds of 15-20 m/s and then exited onto the runout area where it decelerated. The variations in maximum speed were due mainly to the varying condition of the polyethylene lined slope. The sun shining on the plastic caused the snow beneath it to melt, and this material then refroze at night. Over a period of several weeks this process increased local irregularities in the track which then retarded the flow. As the speed of the flow reached about 10 m/s, a powder cloud was observed to form. This made observation of the main flowing mass difficult. Because of this cloud, the depth of flow could not be measured, but was estimated to be about 30 cm at the entrance to the runout area. Deceleration of the snow continued in the runout area until the flow finally stopped. Total runout distances ranged from 14-21 m depending upon the inflow velocity. This motion was recorded on 16 mm motion picture film which was then analyzed. Again, the powder cloud obscured the motion of all but the very front of the flowing snow (Figure 7). Analysis of the film provided only position data on the leading edge as a function of time. Upon coming to rest, the debris depth distribution was measured as a function of position. The maximum debris depth was generally 20 - 25 cm and the length of the debris was usually about 10 m. Beyond 10 m there was a minimal amount of snow of less than 5 cm depth deposited all the way back to the runout entrance. The dump dimensions, runout position



Figure 7: POWDER CLOUD.

versus time, and debris distribution for a typical test are shown in Figures 8,9 and 10. This particular test will be used as the prototype for calibration of the flow models discussed in Chapter 5.

The debris distribution for each test was cross-sectioned to determine the locations of the dyes that were inserted in the snow prior to release. It was generally found that the dye maintained the same relative position in the debris that existed in the released snow. For example, the debris dye locations for the release shown in Figure 7 are plotted in Figure 11. In this figure the distribution of the different colored dyes in the debris pile is shown where concentrations were greatest. The red dye which started at the back and bottom of the dump ended up with some dye on the surface of the debris near the 15.0m position and then penetrated into the snow until maximum concentration was observed at station 14.0 near the bottom of the debris. The blue dye, which started at the bottom front of the released snow, ended up as a ribbon of snow dyed blue 1 to 5 cm thick at the bottom of the debris extending from the front to the rear of the entire debris profile. There was also a concentration of blue dye near the bottom front of the debris near Station 18. The spreading of dye, initially at the front edge of the flow, to the entire length of the runout zone was observed in other tests as well. In addition, a thin layer about 1.0 cm in thickness of snow dyed blue was left trailing the debris all the way back to the entrance of the runout zone.

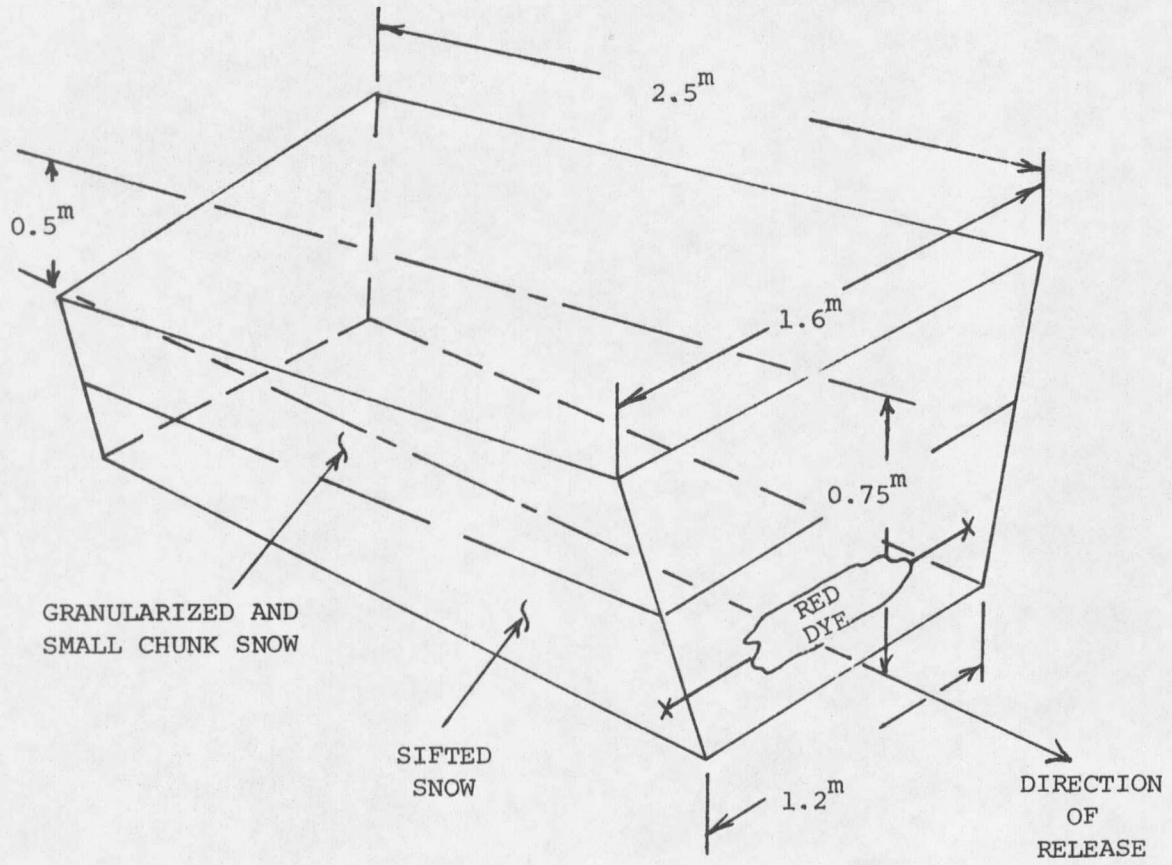


Figure 8: DUMP GEOMETRY, TEST NO. 2-2-23-80.

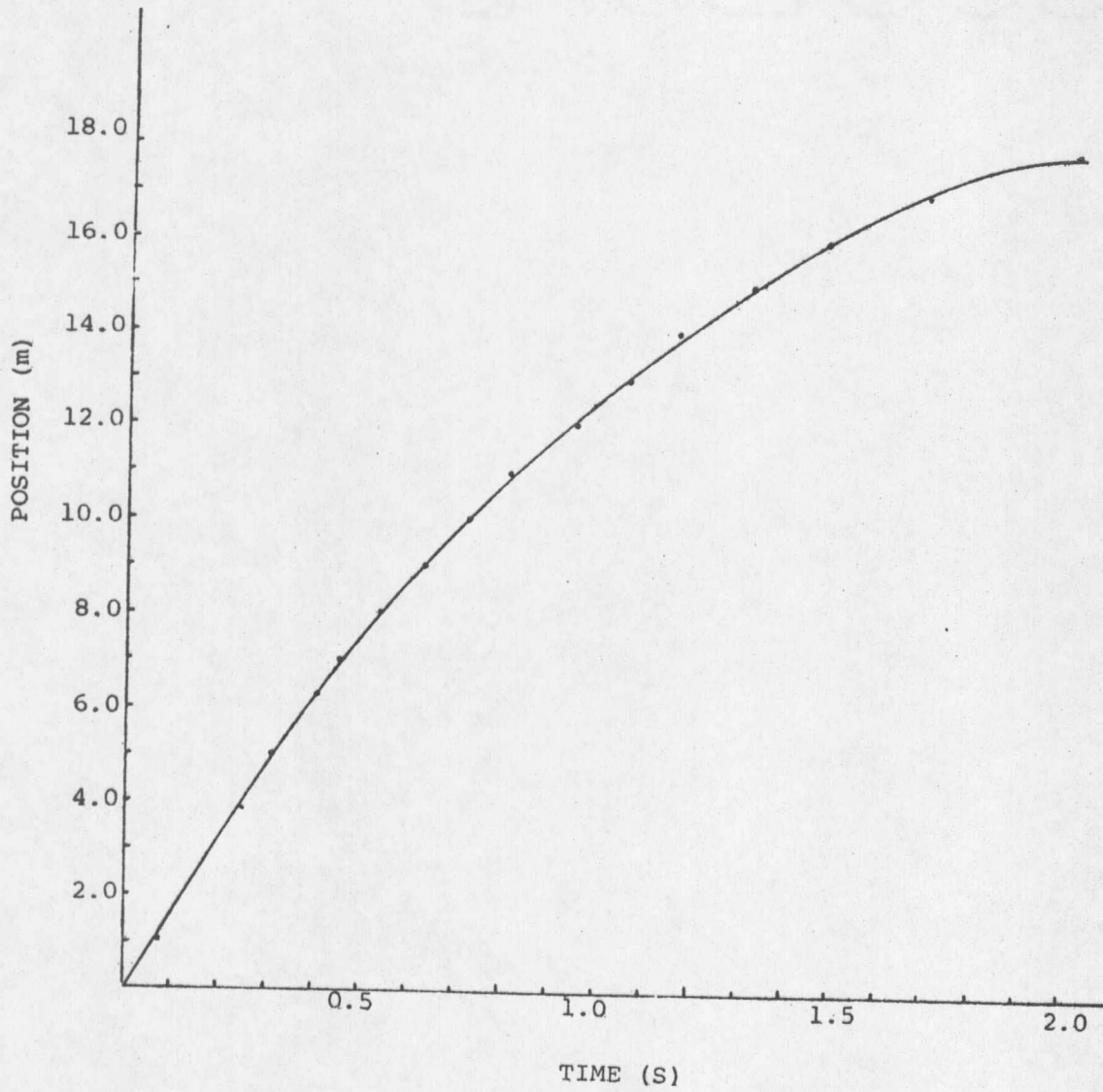


Figure 9. LEADING EDGE POSITION VERSUS TIME FOR TEST NUMBER 2-2-23-80.

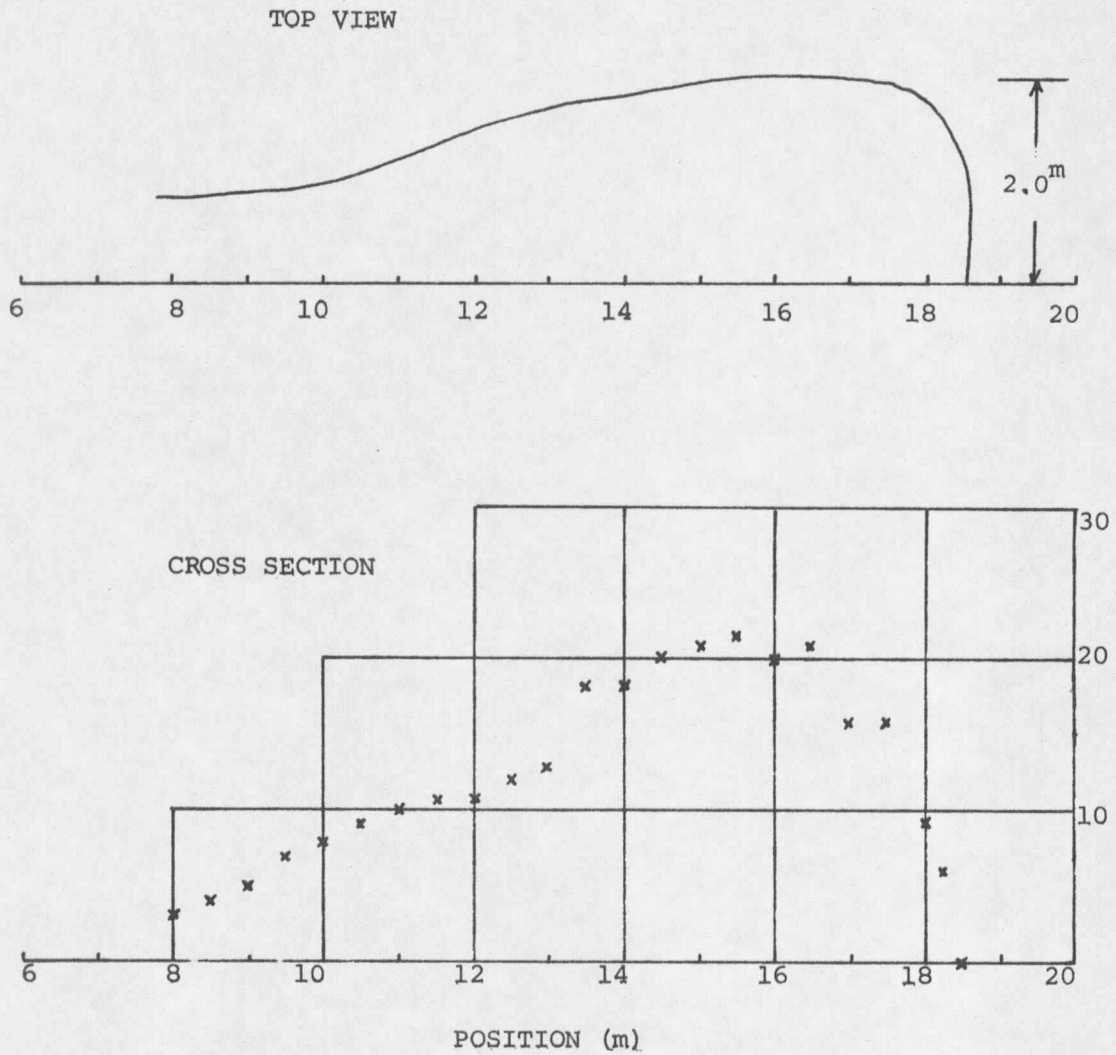


Figure 10: DEBRIS DISTRIBUTION TEST NO. 2-2-23-80.

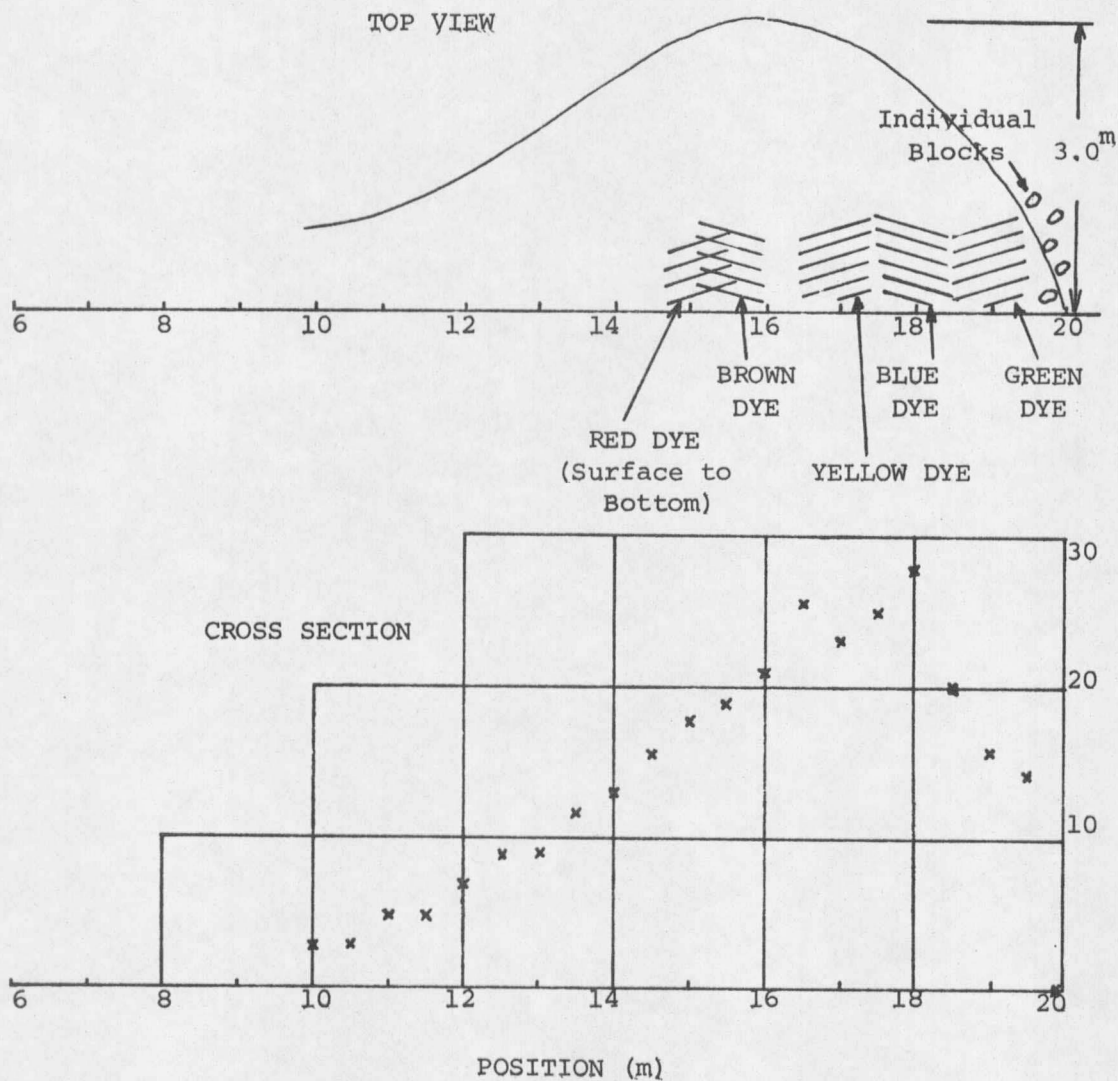


Figure 11: DEBRIS DISTRIBUTION TEST NO. 3-2-23-80.

For the majority of tests, including those discussed above, the release mass was made up of snow sifted through a 6 mm wire mesh to at least a depth of 30 cm. The upper half of the release mass was then made up of granularized snow with some interspersed blocks of up to 5 cm maximum dimension. In another series of tests, considerable effort was taken to fill the release box with individual snow blocks with a minimum of interstitial granular snow. Large blocks of snow were taken from the mid-winter sintered snowpack and cut by a shovel into smaller blocks with maximum dimensions between 10 and 20 cm. These blocks were individually placed in the dump box, with the estimated granular snow residue being less than 5% of the total snow content. Overall dimensions of the release dump and location of local concentrations of dye for a typical chunk test are shown in Figure 12. Outflow of the main body of snow for this test extended to 14.0 m, with individual snow blocks projecting out to 18.0 m (Figure 13). The movement of dye was similar to that observed in other tests. In this case, the brown and blue dyes remained localized on the surface, the green dye stayed in the trailing section and the red dye extended as a ribbon over the length of the debris at the bottom. The yellow block placed on the surface remained on the surface of the debris after the test. In examining the content of the debris pile, it was found that no solid blocks extended down to the runout surface, and the snow at the bottom of the debris was all granular. Blocks that were deposited on the

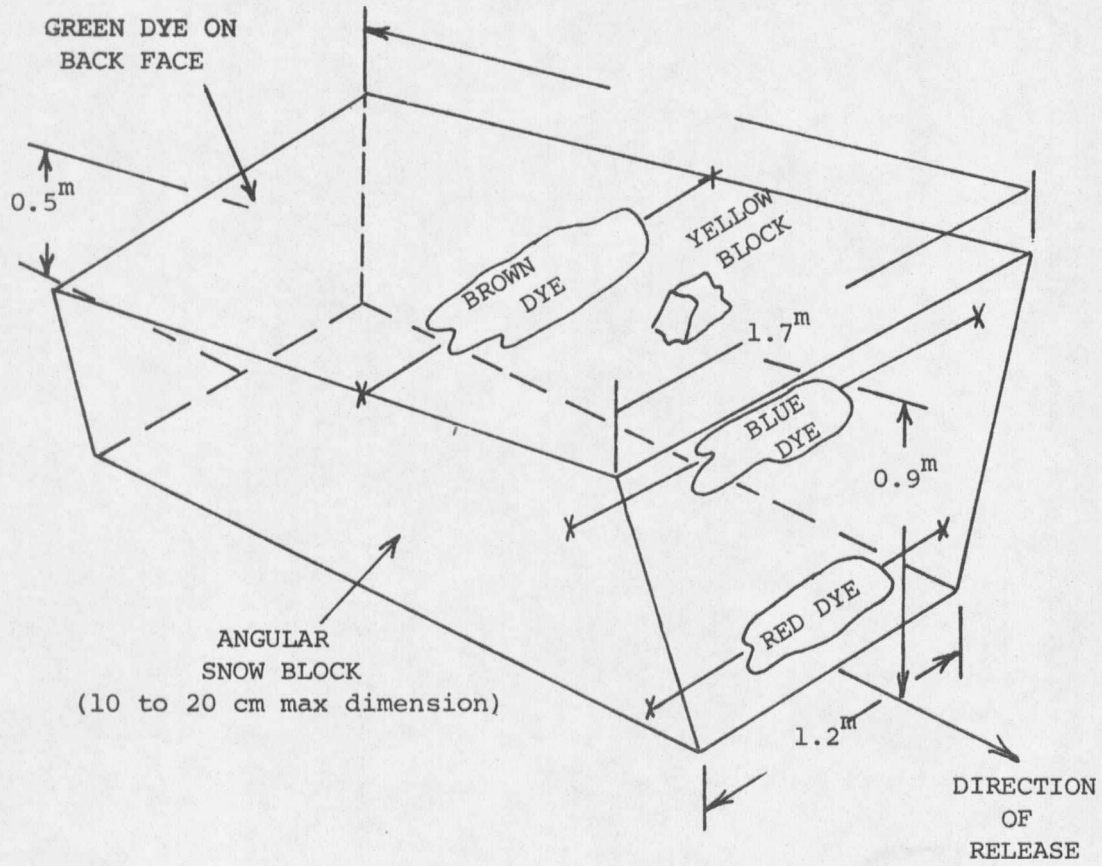


Figure 12: DUMP GEOMETRY, TEST NO. 1-2-25-80 (Block Test).

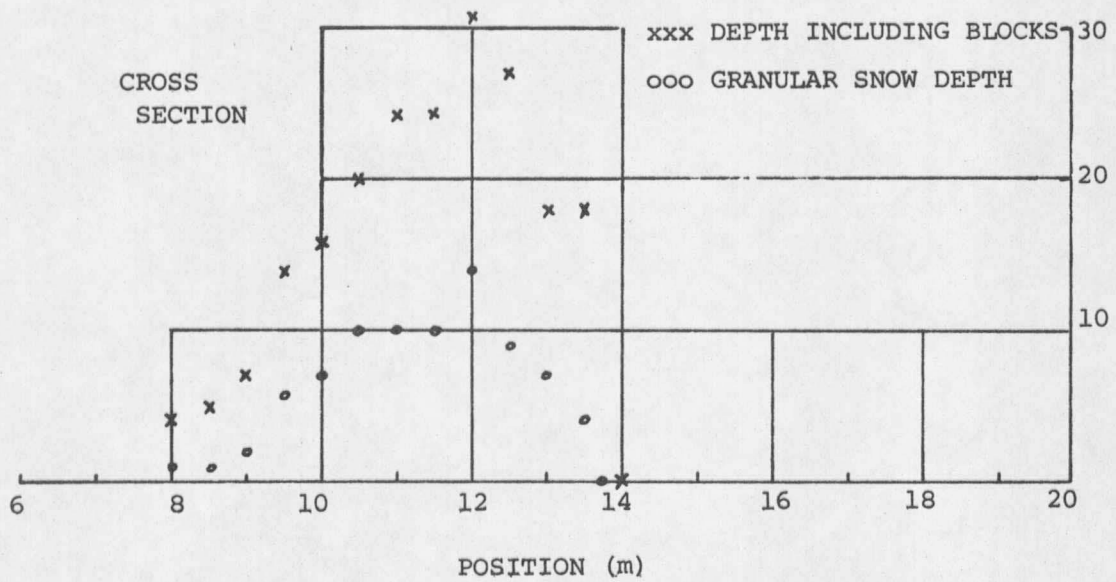
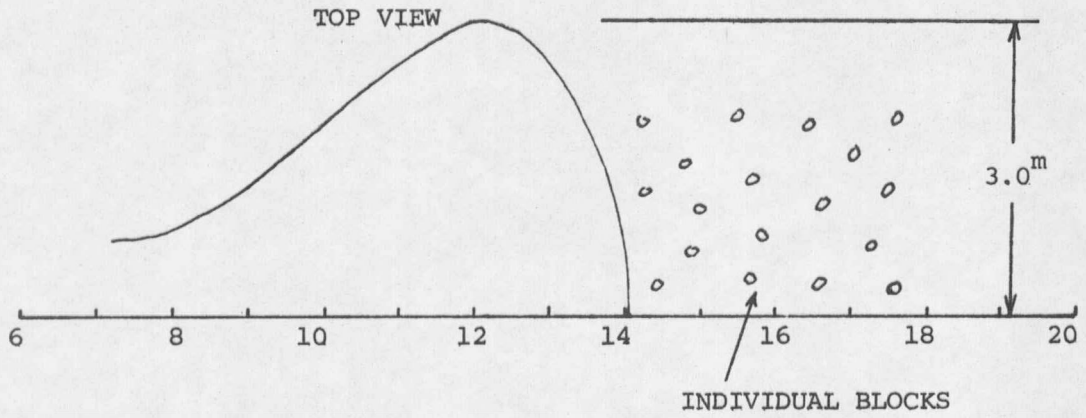


Figure 13: DEBRIS DISTRIBUTION TEST NO. 1-2-25-80.

surface retained their angular shapes, while blocks that were found interspersed with granular snow buried in the debris were small and rounded showing considerable wear and abrasion. Figures 14 and 15 are photographs of the debris cross-section showing this snow distribution. The average depth of the surface of the debris, including blocks, was recorded and then the blocks were removed and the depth of the granularized snow was measured. This information is plotted in Figure 13.

Window Tests

In a number of granular snow tests, the motion of the flowing snow was photographed from behind a glass window inserted in the wall near the entrance of the runout area. This enabled the measurement of the flow velocity as a function of depth in the flow. Figure 16 shows the resulting velocity profile as measured from several tests. These measurements were only taken 0.1 to 0.2 seconds into the flow past the window to minimize the effects of deceleration of the snow. These results show a strong velocity gradient near the lower surface and a nearly uniform velocity for the upper 75% of the flowing snow. The dashed line in the figure is an exponential curve fit to the data.

Discussion of Test Results

In examining the test results, several conclusions can be made. First, there is little mixing or relative motion in the upper depths of the flow. Dye that started on the surface in tests was found to still

